Copy
RM L56G19a

NACA RM L56G19a

C.1

RESEARCH MEMORANDUM

WIND-TUNNEL INVESTIGATION AT HIGH SUBSONIC SPEEDS OF DRAG AT 0° ANGLE OF ATTACK OF SWEPT-WING—FUSELAGE MODELS WITH PYLON-MOUNTED AND SEMISUBMERGED MISSILES

By Thomas J. King, Jr.

Langley Aeronautical Laboratory
Langley Field, Va.

CLASSIFIED DOCUMENT

NATIONAL ADVISORY COMMITTEE
FOR AERONAUTICS
WASHINGTON
October 8, 1956

NACA RM L56G19a

NATIONAL ADVISORY COMMITTEE FOR AERONAUTICS

RESEARCH MEMORANDUM

WIND-TUNNEL INVESTIGATION AT HIGH SUBSONIC SPEEDS OF DRAG AT 0° ANGLE OF ATTACK OF SWEPT-WING—FUSELAGE MODELS WITH PYLON-MOUNTED AND SEMISUBMERGED MISSILES

By Thomas J. King, Jr.

SUMMARY

A wind-tunnel investigation was made at Mach numbers from 0.50 to 0.96 of the drag at 0° angle of attack of two wing-fuselage models having 45° sweptback wings and various missile arrangements. One model had missiles suspended from pylons beneath the wing; on the other model the missiles were semisubmerged in the sides of the fuselage. For the pylon-mounted arrangements, two missiles were located symmetrically at 49 percent of the wing semispan and were tested on two sizes of pylons. The semisubmerged missile configurations consisted of arrangements of two and four missile models mounted on a flat-sided fuselage with the wing in a high position. The semisubmerged missiles were simulated by half-missile models attached to the fuselage sides; no evaluation was made of effects of gaps between the missiles and the fuselage or of fuselage cavities which would be exposed after disposition of the missiles.

The results show that two semisubmerged missiles in a forward location on the fuselage increased the total drag a maximum of about 8 percent compared to a maximum increase in model drag of about 50 percent on a wing-fuselage model with two pylon-mounted missiles. The maximum increase in model drag due to pylon-mounted missiles was equivalent to more than seven times the drag of the isolated missiles. Reducing the pylon chords and thickness by one-half and moving the pylons and missiles forward reduced the total model drag by as much as 15 percent over the Mach number range investigated.

INTRODUCTION

The National Advisory Committee for Aeronautics is making investigations on airplane and missile models to provide a better understanding of the problems brought about by the external carriage of missiles on

airplanes. Results at high subsonic speeds of some effects of adding various combinations of missiles on longitudinal stability and performance of wing-fuselage models are presented in reference 1. The present paper presents drag results at high subsonic speeds for wing-fuselage models mounting missiles on pylons and missiles semisubmerged in a fuselage. The investigation was made at subsonic Mach numbers from 0.50 to 0.96 in the Langley high-speed 7- by 10-foot tunnel.

SYMBOLS

C_D	drag coefficient of wing-fuselage model, $\frac{\text{Drag}}{qS}$
ΔC_D	installation drag coefficient, $\left(C_D\right)_{\text{model + missiles}} - \left(C_D\right)_{\text{model}}$
$C_{D,m}$	missile drag coefficient based on missile body frontal area, $\frac{\text{Drag}}{qA}$
S	wing area of wing-fuselage models, sq ft
A	maximum frontal area of missile body, sq ft
$\frac{A}{S}$	ratio of maximum frontal area of missile body to wing area of wing-fuselage model, 0.00102
$\bar{c}$	mean aerodynamic chord of wing, $\frac{2}{S}\int_0^{b/2} c^2 dy$, ft
c	chord, ft
b	wing span, ft
y	spanwise distance from plane of symmetry of wing-fuselage model, ft
d	diameter of fuselage of model A, ft
h	semiwidth of fuselage of model B, ft
x	longitudinal distance from missile body nose, ft
r	radius of missile body, ft

l	fuselage length, ft
l_m	missile body length, ft
q	dynamic pressure, $\frac{\rho V^2}{2}$, lb/sq ft
ρ	air density, slugs/cu ft
μ	absolute coefficient of viscosity, lb-sec/sq ft
V	airstream velocity, ft/sec
M	Mach number
R	Reynolds number
α	angle of attack relative to fuselage center line, deg

Subscripts:

b	base
by	bouyancy
max	maximum
m	missile
p	pylon
w	wing

MODELS AND APPARATUS

Two sting-mounted wing-fuselage models, various missile models, and a sting-mounted missile model were used for the present investigation. A three-view drawing of wing-fuselage model A, which was tested with pylon-mounted missiles, is presented in figure 1. The wing was constructed of aluminum alloy and was mounted with the wing-chord plane on the fuselage center line. Ordinates of the fuselage, which also was made of aluminum alloy, are presented in table I. Also presented in figure 1 are sketches of the complete-missile-pylon arrangements tested. The missiles on the large pylons were also tested with wings off, with tail fins off, and with wings and tail fins off. The missiles were mounted such that the planes of the wings and fins were oriented at 45°

to the vertical and horizontal. Geometric details of the missile models are given in figure 2. The missiles had aluminum-alloy bodies and steel wings and tail fins. Ordinates of the pylon cross sections are given in table II. The large pylons had chord lengths of 6.14 inches and were mounted with the leading edges 1.09 inches rearward of the wing leading edge. The small pylons had chord lengths of 3.07 inches and were mounted with the leading edges coinciding with the wing leading edge.

The drag of one missile in the presence of a large pylon and mounted on wing-fuselage model A was obtained with the setup shown in figure 3. The missile body housed a strain-gage balance which was attached to the pylon by means of a small strut.

Wing-fuselage model B, which is shown in figure 4, was employed to investigate semisubmerged missile installations. Model B mounted on the sting-support system in the Langley high-speed 7- by 10-foot tunnel is shown in figure 5(a). The aluminum-alloy wing was mounted 2.00 inches above the fuselage center line. Ordinates of the fuselage are presented in table III. The semisubmerged missiles were simulated with models of half missiles having one wing panel and one tail fin (fig. 5(b)). The missile bodies were made of brass and wing and tail surfaces were made of steel. The missile models were attached to the fuselage sides with the planes of the wings and tail fins horizontal. Simulation of fuselage cavities or gap between missiles and fuselage was not attempted.

Drag of an isolated sting-mounted missile model was obtained on the model shown in figure 6. The missile fuselage was made of plastic and the wings and tails were made of steel. The missile was mounted on an internal strain-gage balance connected to the sting.

Diagrams of the longitudinal-area distributions of models A and B with missile arrangements are presented in figure 7.

TESTS AND CORRECTIONS

The tests were made in the Langley high-speed 7- by 10-foot tunnel. Drag measurements of the wing-fuselage models and the sting-mounted missile model were made at $\alpha = 0^{\circ}$ over the ranges of Mach numbers shown as follows:

Model	M
Model A with pylon-mounted missiles	0.50 to 0.94
Model B with semi-submerged missiles	0.50 to 0.96
Isolated missile	0.50 to 0.98

The variations of Reynolds number with Mach number of the wing-fuselage models and of the missiles are presented in figure 8. The wing-fuselage models and the isolated missile model were tested in conditions of free transition. Model A had been previously tested in numerous investigations and consequently had comparatively rougher surfaces than model B which had a new fuselage and a relatively new wing. The surfaces of the missile models were very similar in degree of smoothness, and calculation of the skin friction drag coefficient (ref. 2) indicates that both sizes of missile models should experience essentially all-turbulent boundary-layer flow.

Blocking corrections determined by the method of reference 3 were applied to Mach number and dynamic pressure.

Bouyancy corrections determined from the static-pressure gradient that exists along the tunnel center line were added to the wing-fuselage drag results. The bouyancy corrections to the drag are shown in the following table:

M	$C_{D,by}$ for -	
	Model with pylon-mounted missiles	Model with semisubmerged missiles
0.50	0.0015	0.0021
.80	.0016	.0022
.90	.0018	.0025
.94	.0018	.0026
.96		.0026

Bouyancy corrections to the drag of the isolated missile were evaluated but were not applied to the results. The bouyancy correction $C_{D,m,by}$ was approximately 0.010 (less than 3 percent $C_{D,m}$) over the range of Mach numbers investigated.

[redacted]

The drag data of the wing-fuselage models have been adjusted to correspond to a pressure at the base of the fuselages equal to free-stream static pressure. Base-drag coefficients of the wing-fuselage models are presented in figure 9. The presence of the missiles on the wing-fuselage models has essentially no effect on the base-drag coefficients (ref. 4). Base-drag coefficients of the isolated missile model also are presented in figure 9 but these were not applied to the isolated missile drag coefficients presented.

Estimated maximum errors in the experimental drag coefficients resulting from reading, recording, and measuring equipment errors are presented in the following table:

M	C_D for models A and B	$C_{D,m}$ for -	
		Isolated missile	Missile in presence of pylon, wing, and fuselage
0.50	±0.0007	±0.025	±0.020
.70	.0004	.015	.012
.80	.0004	.013	.010
.90	.0003	.011	.009
.94	.0003	.011	.008
.98	-------	.010	------

The accuracy of faired values of C_D and values of ΔC_D obtained from faired C_D curves is believed to be better than indicated by the estimated values in the preceding table.

PRESENTATION OF RESULTS

The results of the investigation are presented in the following figures:

	Figure
Drag of model A without and with pylon-mounted missiles	10
Drag of isolated missile and missile in presence of pylon, wing, and fuselage	11
Comparison of installation drag of two pylon-mounted missiles, drag of two isolated missiles, and twice drag of missile in presence of model	12
Effect of missile components and pylons on installation drag	13

Figure

Drag of model B without and with semisubmerged missiles 14
Comparison of installation drag of pylon-mounted and semi-submerged missiles 15

DISCUSSION

The results presented herein were obtained on two wing-fuselage models of differing geometry and wing arrangements. (See figs. 1 and 4.) The differences in the two models are also reflected in the longitudinal area distributions presented in figure 7. In the section entitled "Tests and Corrections" it was pointed out that there were differences in the degree of surface smoothness of the two wing-fuselage models. In view of the dissimilarities in the models it is to be expected that the results are comparable in a qualitative sense only, particularly at high-subsonic speeds.

Pylon-Mounted Missiles

Drag coefficients of model A at $\alpha = 0^\circ$ without and with pylon-mounted complete missiles are presented in figure 10. The missiles were mounted on pylons located at $\frac{y}{b/2} = 0.49$. One set of missiles was mounted from large (long chord) pylons which placed the missile wings beneath the model wing. A second arrangement with small (short chord) pylons positioned the missiles such that the missile wings were ahead of the model wing (fig. 1). Referring to figure 10, the drag of the small-pylon arrangement was from 5 to 15 percent less than the drag of the large-pylon configuration. The missile—large-pylon configuration increased the model drag a minimum of about 17 percent ($M = 0.70$) which compares with the 7-percent increase ($M = 0.50$) of the missile—small-pylon configuration. Either arrangement of missiles and pylons on the model decreased the drag-rise Mach number; at $M = 0.94$ the missile—large-pylon configuration had approximately 50 percent more drag than the clean wing-fuselage model.

Drag of a missile in the presence of a large pylon, wing, and fuselage (fig. 4), and drag of an isolated missile (fig. 8) are presented in figure 11. Above $M = 0.80$ the drag of the missile in the presence of the model increases rapidly and is approximately twice the isolated missile drag at $M = 0.94$.

The installation drag of the configuration with one missile mounted from a pylon under each wing (2 missiles), the drag of two isolated

missiles, and twice the drag of the missile in the presence of a large pylon, wing, and fuselage (all coefficients based on model-wing area) are compared in figure 12. The minimum installation drag of the pylon-mounted missile configuration was more than twice the drag of the isolated missiles; at $M = 0.94$, ΔC_D was more than seven times the drag of two isolated missiles.

Installation-drag coefficients of configurations of pylons and missiles (with and without wings and tail fins) located symmetrically at $\frac{y}{b/2} = 0.49$ (fig. 1) are presented in figure 13(a). At low Mach numbers the installation drag of the arrangement with pylons and missiles' bodies was from about one-fifth to one-fourth of the installation drag of the complete missiles with pylons.

Installation drag due to pylons only is presented in figure 13(b). At low Mach numbers ΔC_D due to the pylons was zero or negative but increased to 51 and 36 percent of the missiles-on installation drag (large and small pylons, respectively) at $M = 0.94$. It is to be noted that the present results are for pylons at two different longitudinal locations (fig. 1) and thus show combined effects of pylon size and longitudinal location.

Semisubmerged Missiles

Drag coefficients at $\alpha = 0^\circ$ of the wing-fuselage model without and with semisubmerged missiles are presented in figure 14. Two missiles carried in the rearward position (fig. 4) gave the lowest increase in drag. At a Mach number of about 0.90, the drag was increased by about 4 percent by the two rearward semisubmerged missiles compared to an 8 percent increase in drag resulting from two missiles in a forward position. Four semisubmerged missiles increased the drag a maximum of about 13 percent ($M = 0.86$).

Comparisons of the installation drag coefficients of the pylon-mounted missiles on model A and the semisubmerged missiles on model B are made in figure 15. Two semisubmerged missiles in either forward or rearward positions on the fuselage sides produced lower installation drag than either of the two pylon-mounted missile arrangements. The maximum installation drag of the two forward semisubmerged missiles ($M = 0.90$) was equivalent to an 8-percent increase in model drag compared to the 20-percent increase in model drag ($M = 0.90$) due to the better of the pylon-mounted missile configurations (small pylons). Above Mach numbers of about 0.85 to 0.91 the installation drag of all of the semisubmerged missile arrangements decreased with further increase in Mach numbers; in fact, for either arrangement of two semisubmerged missiles, the

installation drag was eliminated at the highest test Mach number (M = 0.96). The installation drag of the pylon-mounted missiles on model A, on the other hand, reached maximum values at the highest test Mach number (M = 0.94).

CONCLUDING REMARKS

An investigation has been made at high subsonic speeds to determine the drag at 0° angle of attack of a wing-fuselage model having symmetrical arrangements of pylon-mounted missiles and of a second wing-fuselage model having missiles semisubmerged in the sides of the fuselage. The results show that two semisubmerged missiles in a forward location on the fuselage increased the total drag a maximum of about 8 percent compared to a maximum increase in model drag of about 50 percent on a wing-fuselage model with two pylon-mounted missiles. The increase in model drag due to pylon-mounted missiles was equivalent to more than seven times the drag of the isolated missiles. Reducing the pylon chords and thickness by one-half and moving the pylons and missiles forward reduced the total model drag as much as 15 percent over the Mach number range investigated.

Langley Aeronautical Laboratory,
National Advisory Committee for Aeronautics,
Langley Field, Va., July 3, 1956.

REFERENCES

1. Silvers, H. Norman, and Alford, William J., Jr.: Investigation at High Subsonic Speeds of the Effect of Adding Various Combinations of Missiles on the Aerodynamic Characteristics of Sweptback and Unswept Wings Combined With a Fuselage. NACA RM L54D20, 1954.

2. Hoerner, Sighard F.: Aerodynamic Drag. Publ. by the author (148 Busteed, Midland Park, N. J.), 1951.

3. Herriot, John G.: Blockage Corrections for Three-Dimensional-Flow Closed-Throat Wind Tunnels, With Consideration of the Effect of Compressibility. NACA Rep. 995, 1950. (Supersedes NACA RM A7B28.)

4. Silvers, H. Norman, and King, Thomas J., Jr.: Investigation at High Subsonic Speeds of Bodies Mounted From the Wing of an Unswept-Wing-Fuselage Model, Including Measurements of Body Loads. NACA RM L52J08, 1952.

TABLE I.- MODEL A FUSELAGE ORDINATES

[Basic fineness ratio 12, actual fineness ratio 9.8 achieved by cutting off rear portion of fuselage]

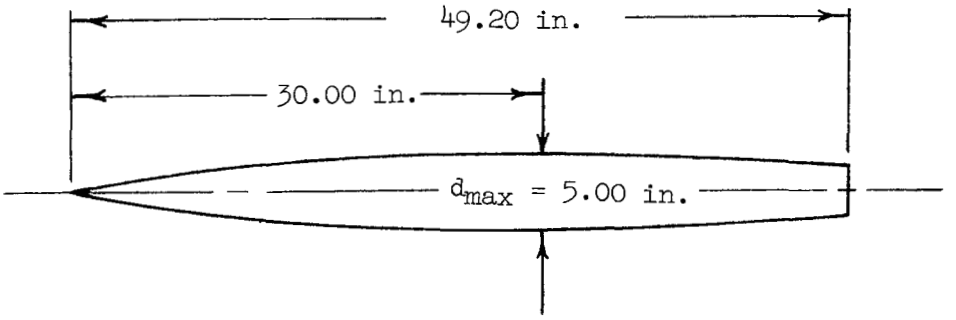

Ordinates, percent length	
Station	Radius
0	0
.61	.28
.91	.36
1.52	.52
3.05	.88
6.10	1.47
9.15	1.97
12.20	2.40
18.29	3.16
24.39	3.77
30.49	4.23
36.59	4.56
42.68	4.80
48.78	4.95
54.88	5.05
60.98	5.08
67.07	5.04
73.17	4.91
79.27	4.69
85.37	4.34
91.46	3.81
100.00	3.35
L. E. radius = 0.0006l	

TABLE II.- PYLON ORDINATES

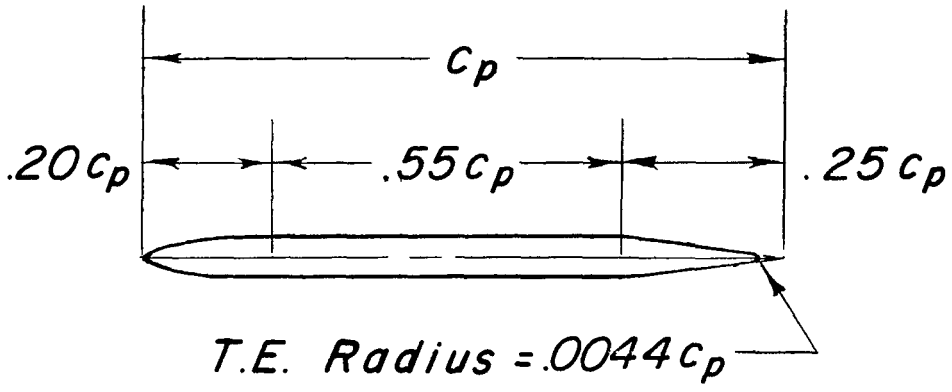

Station	ordinate
0	0
.025	.0146
.050	.0200
.150	.0290
.200	.0300
.750	.0300
Straight line	
1.000	0

TABLE III.- MODEL B FUSELAGE ORDINATES

[Fineness ratio 10.95]

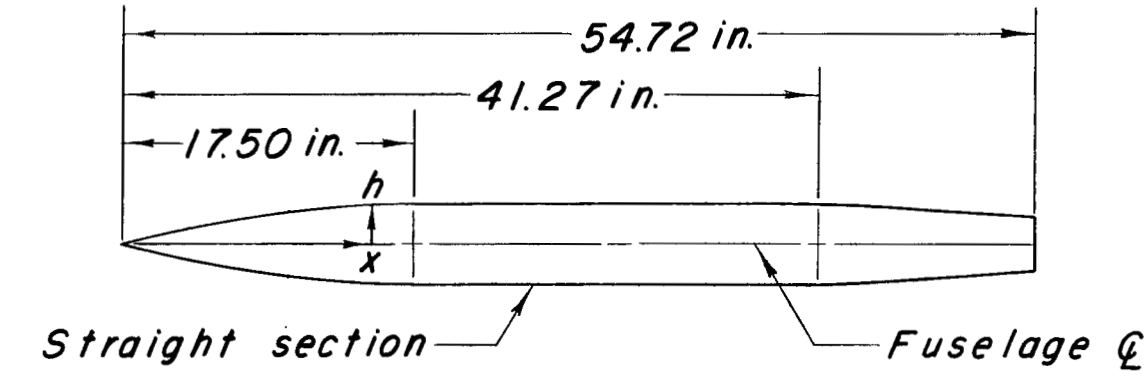

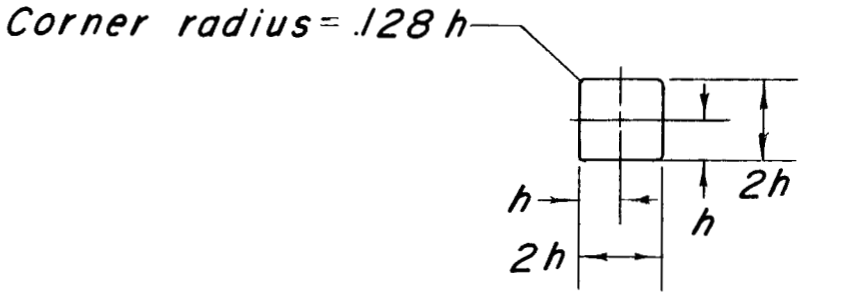

Typical cross section

Profile coordinates, in.	
x	h
0	0
2.00	.53
4.00	1.00
6.00	1.44
8.00	1.80
10.00	2.07
12.00	2.30
14.00	2.42
16.00	2.47
17.50	2.50
41.27	2.50
43.27	2.42
45.27	2.35
47.27	2.25
48.30	2.14
54.72	1.65

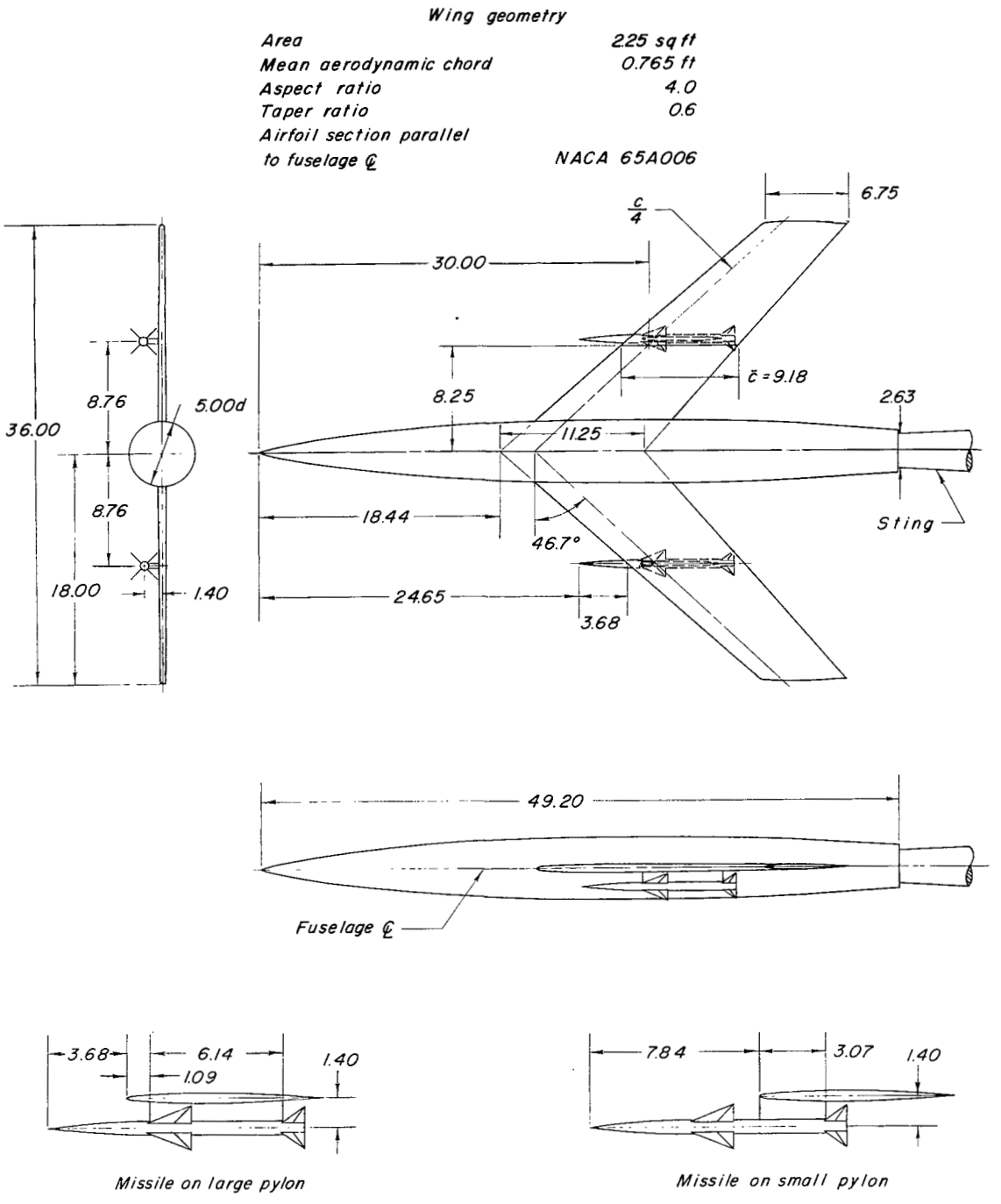

Figure 1.- Three-view drawing of model A with pylon-mounted missiles. All dimensions are in inches unless otherwise noted.

Nose ordinates, in.

x	r
0	0
.500	.075
1.000	.140
1.500	.195
2.000	.241
2.500	.276
3.000	.302
3.500	.318
4.050	.324

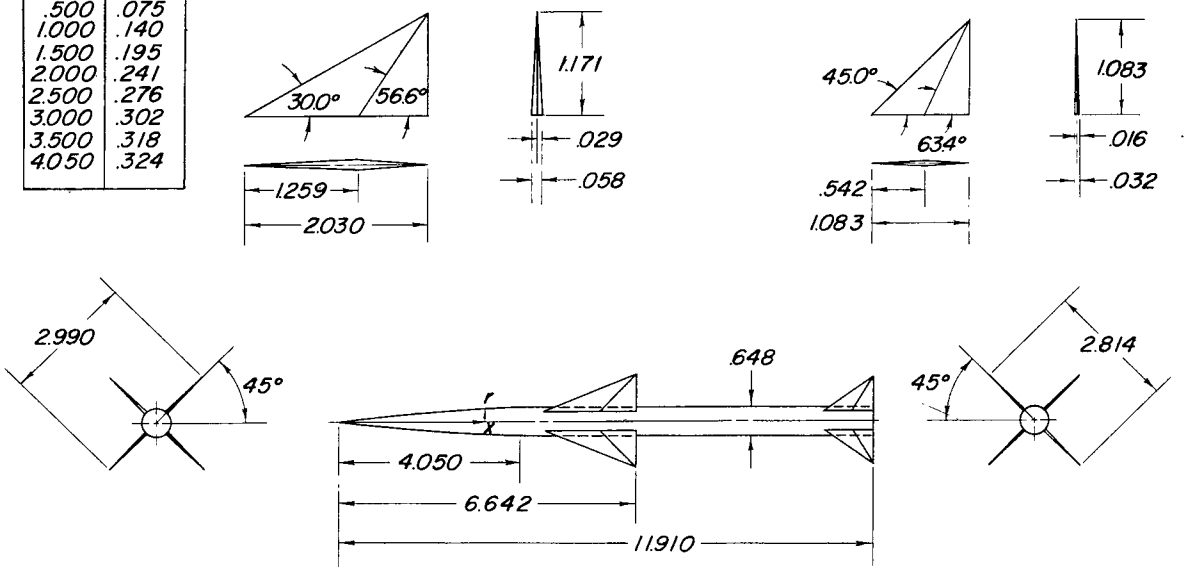

Figure 2.- Details of pylon-mounted missile model. All dimensions are in inches.

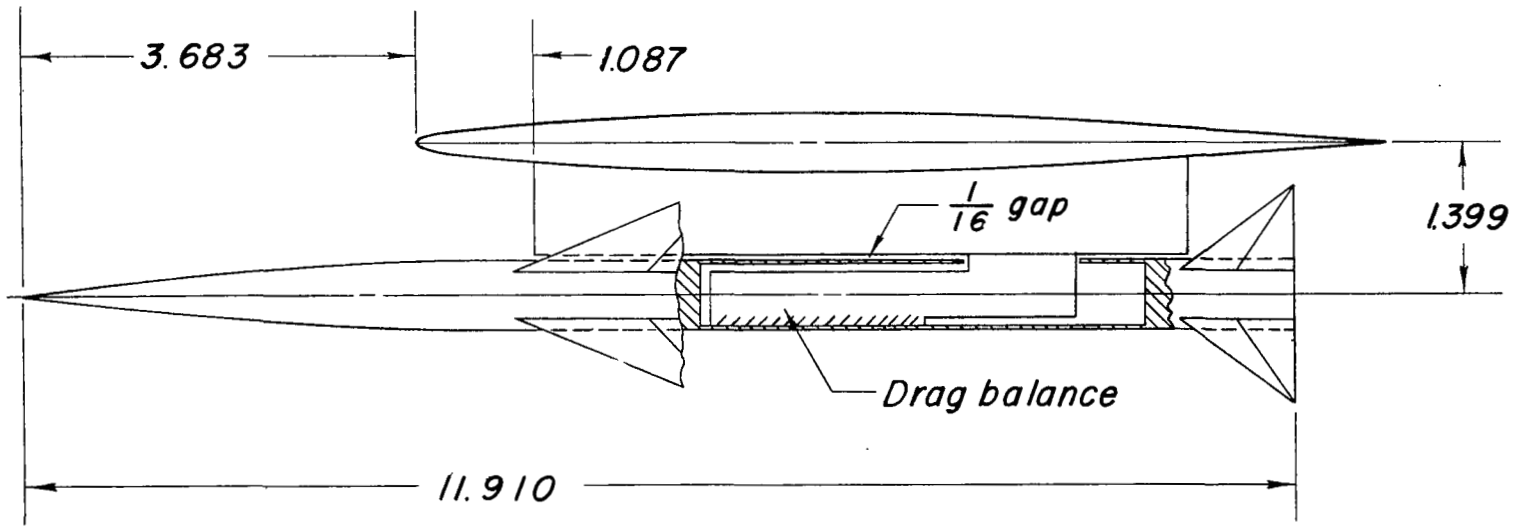

Figure 3.- Cutaway drawing of missile model with internal strain-gage drag balance. All dimensions are in inches.

Wing geometry	
Area	2.25 sq ft
Mean aerodynamic chord	0.822 ft
Aspect ratio	4.0
Taper ratio	0.3
Airfoil section parallel to fuselage ℄	NACA 65A006

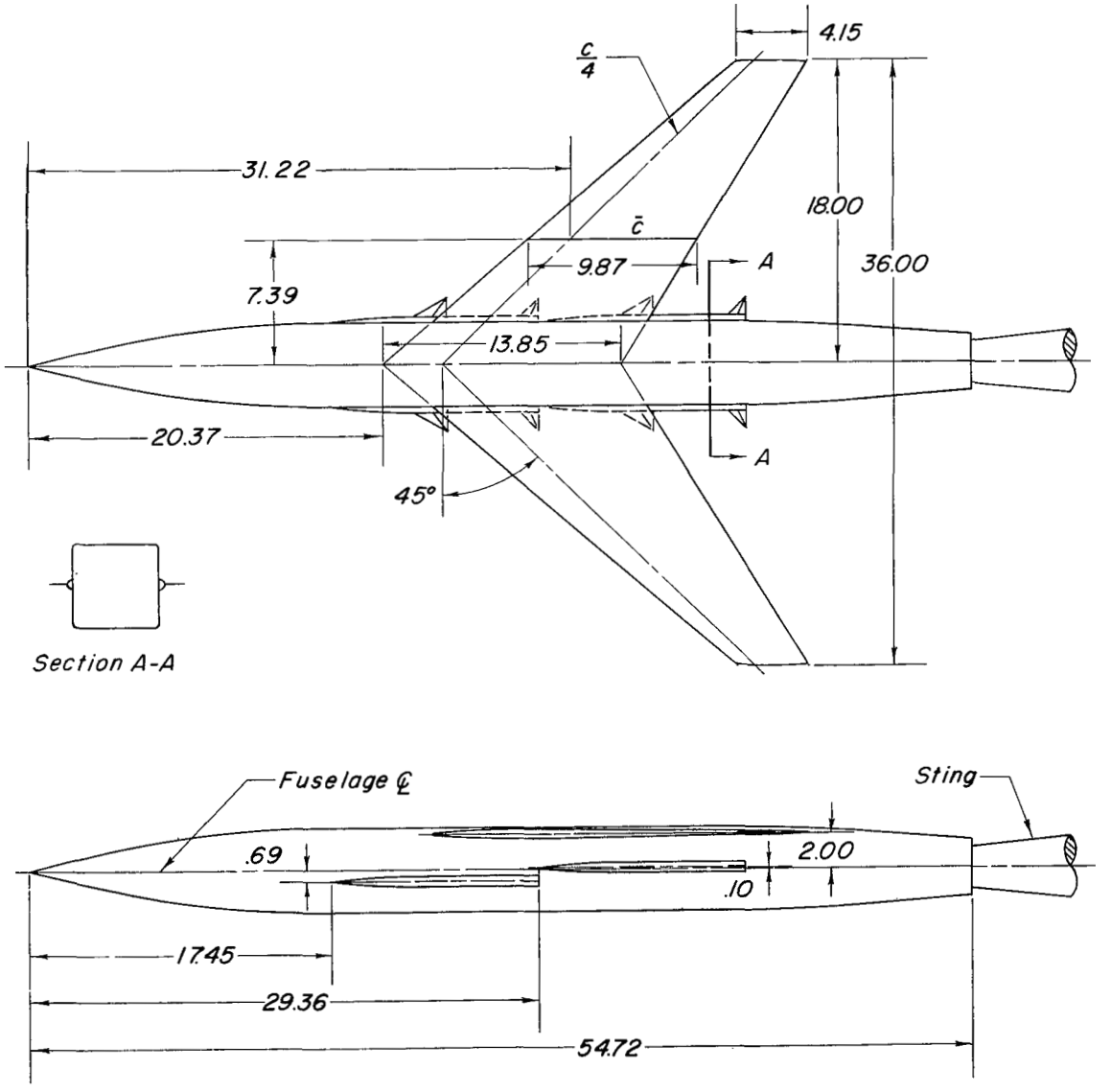

Figure 4.- Two-view drawing of model B with semisubmerged missiles. All dimensions are in inches except where noted.

L-86828

(a) Wing-fuselage.

Figure 5.- Photograph of wing-fuselage model B as tested in Langley high-speed 7- by 10-foot tunnel.

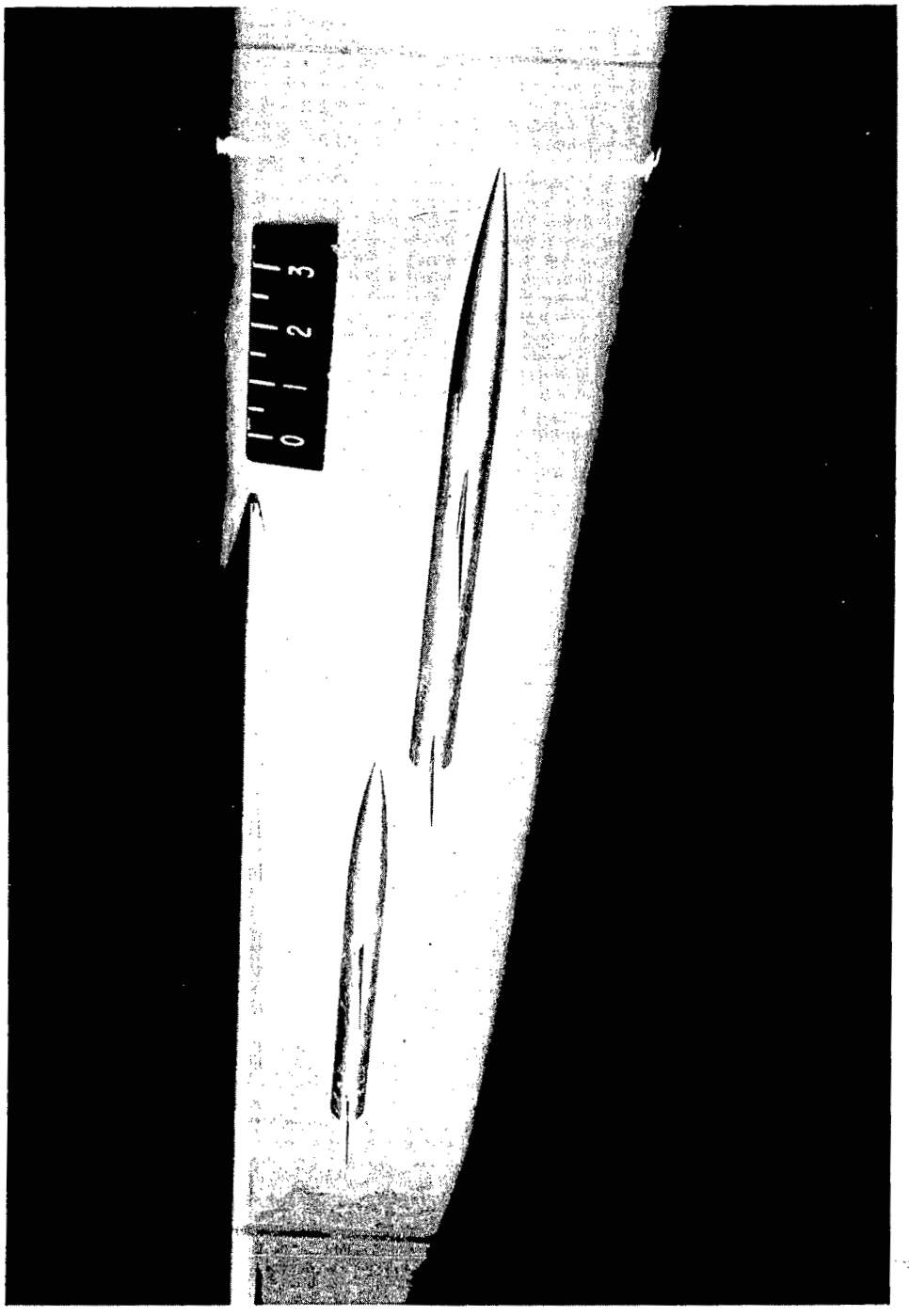

L-86829

(b) Semisubmerged missiles on right side of model.

Figure 5.- Concluded.

Nose ordinates, in.	
x	r
0	0
1.000	.148
2.000	.272
3.000	.373
4.000	.450
5.000	.504
6.000	.533
6.750	.540

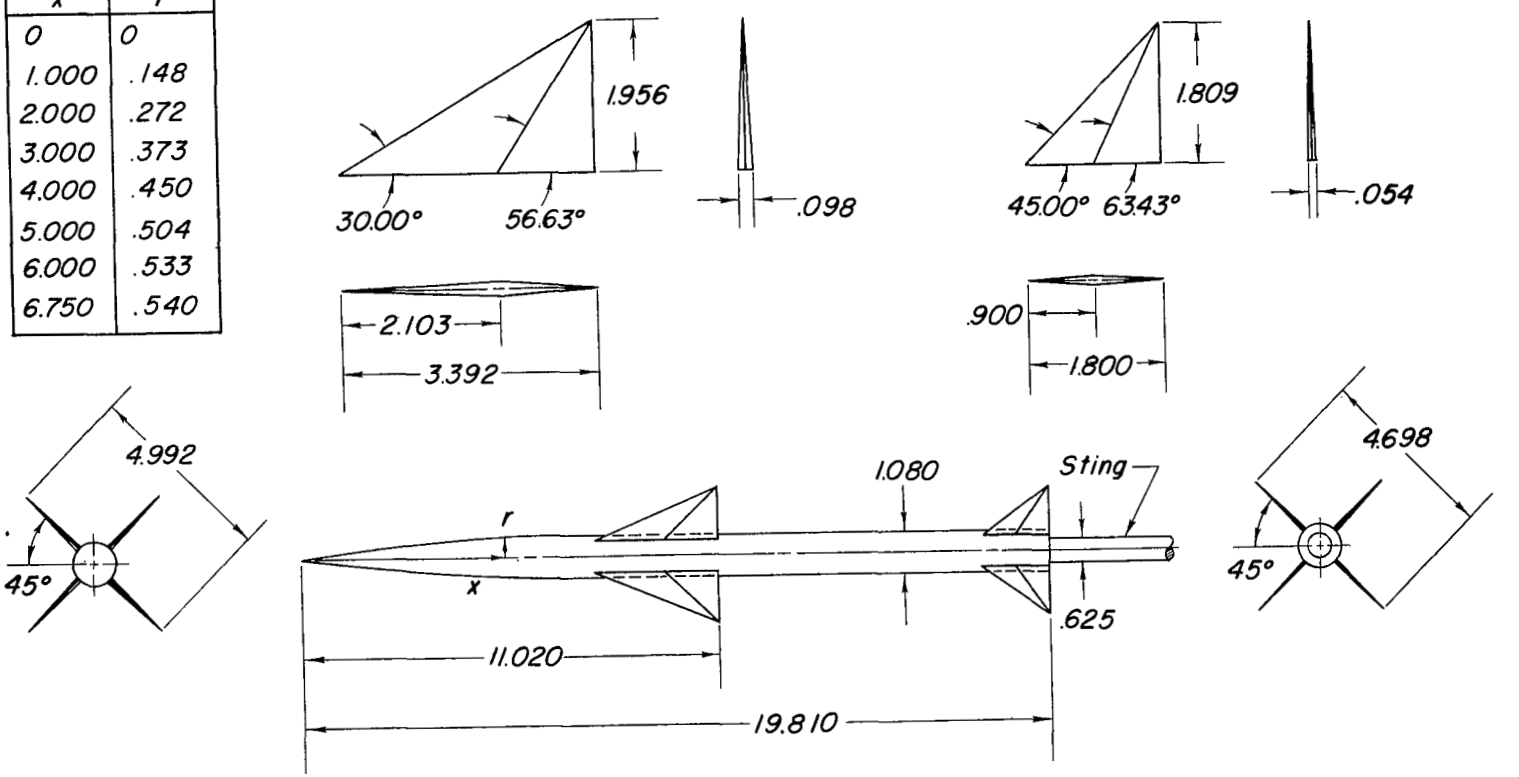

Figure 6.- Details of sting-mounted missile model. All dimensions are in inches.

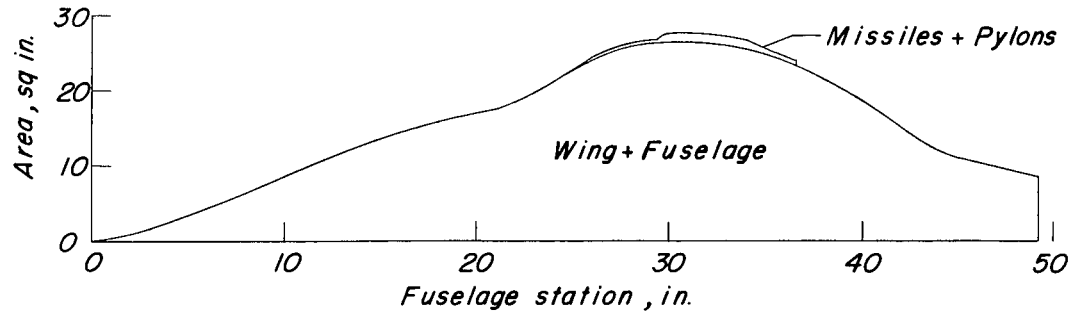

Model A with missiles on large pylons.

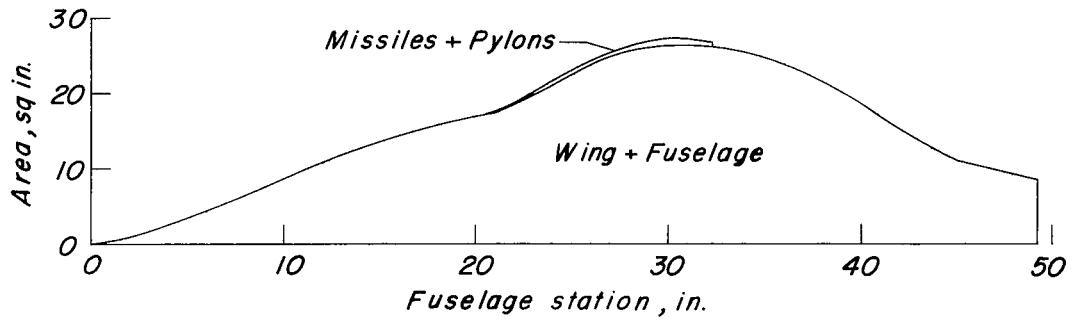

Model A with missiles on small pylons.

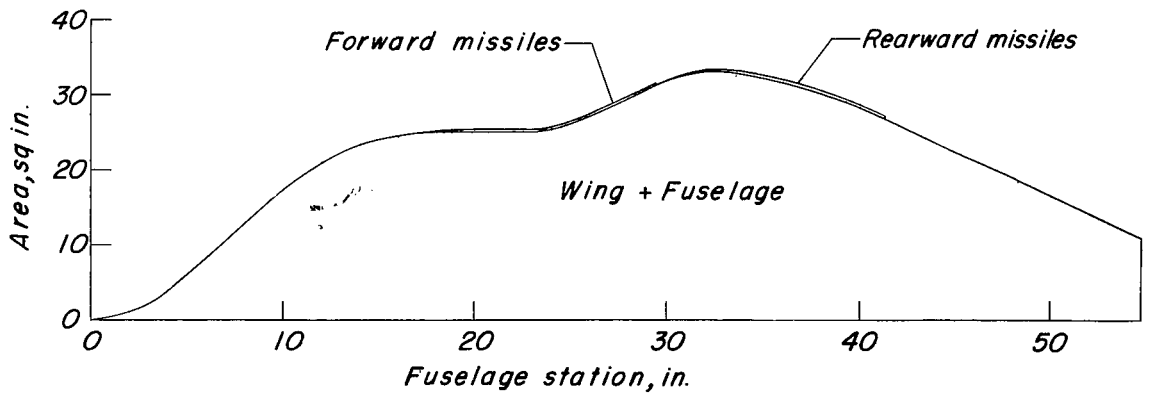

Model B with semisubmerged missiles.

Figure 7.- Longitudinal area distributions of model A with pylon-mounted missiles and model B with semisubmerged missiles.

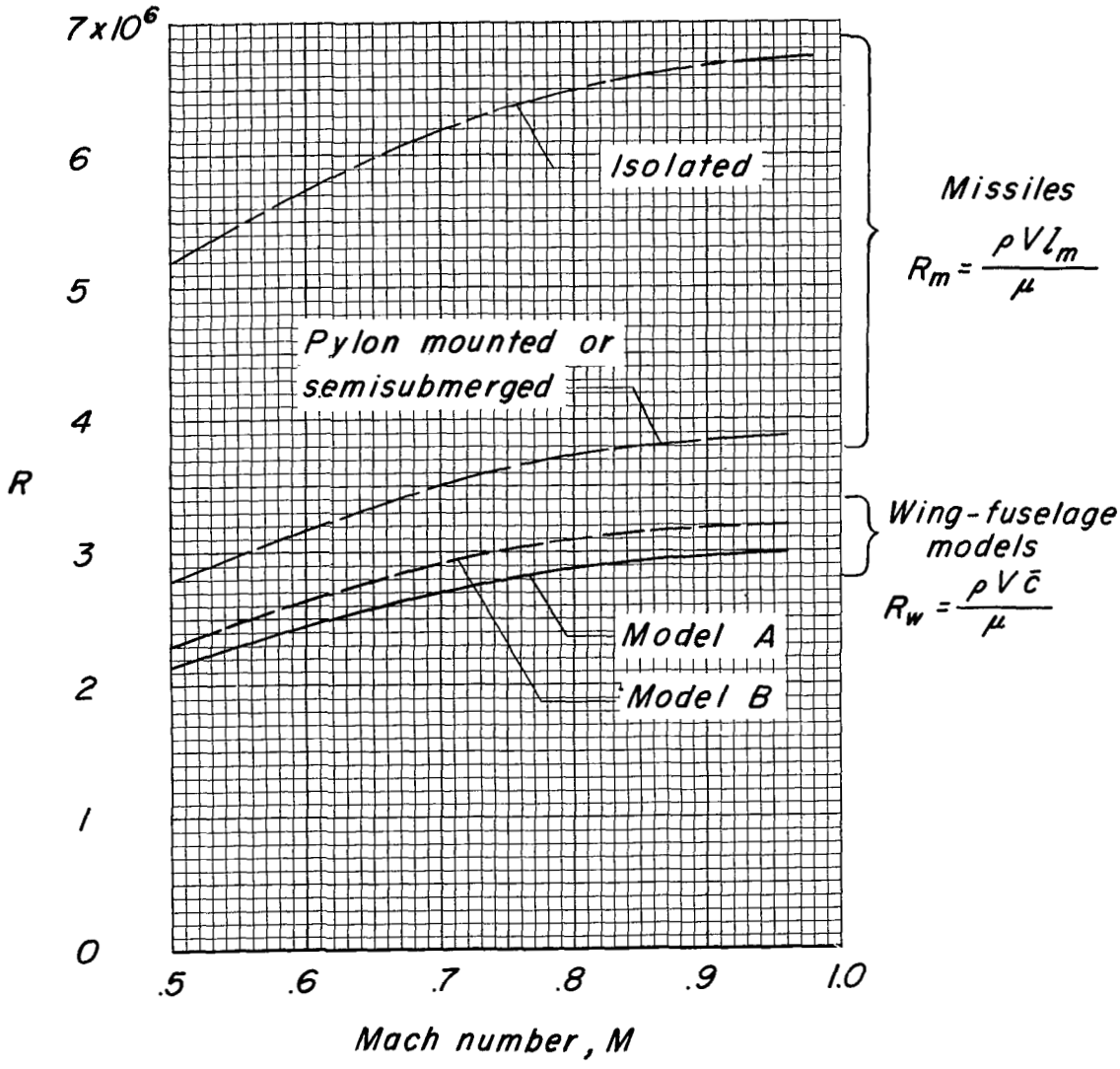

Figure 8.- Variation of Reynolds number with Mach number.

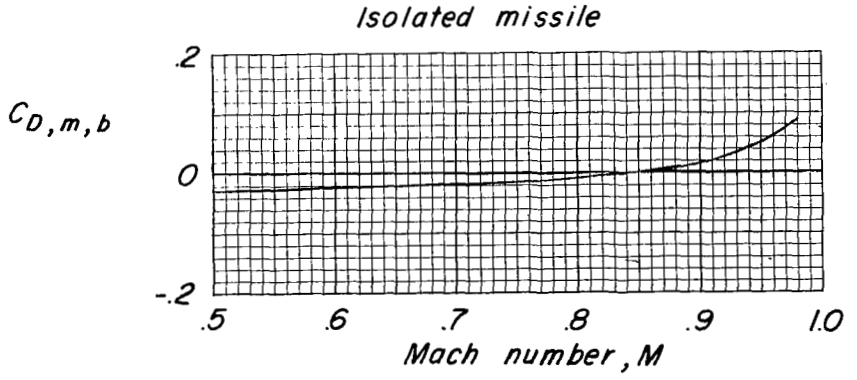

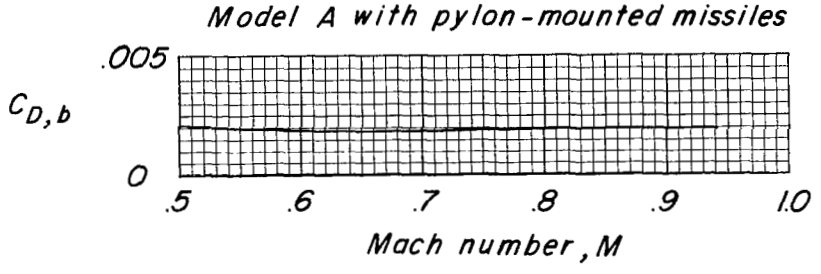

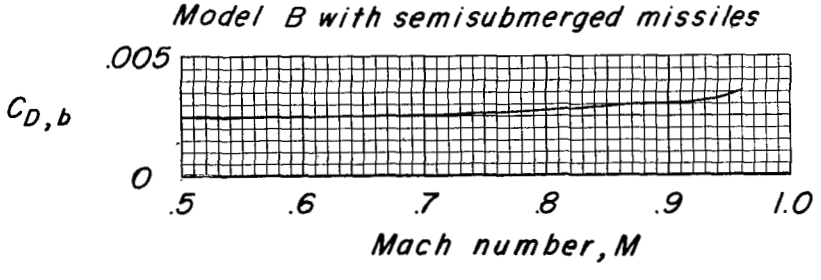

Figure 9.- Variation of base-drag coefficient with Mach number of isolated missile model, model A with pylon-mounted missiles, and model B with semisubmerged missiles.

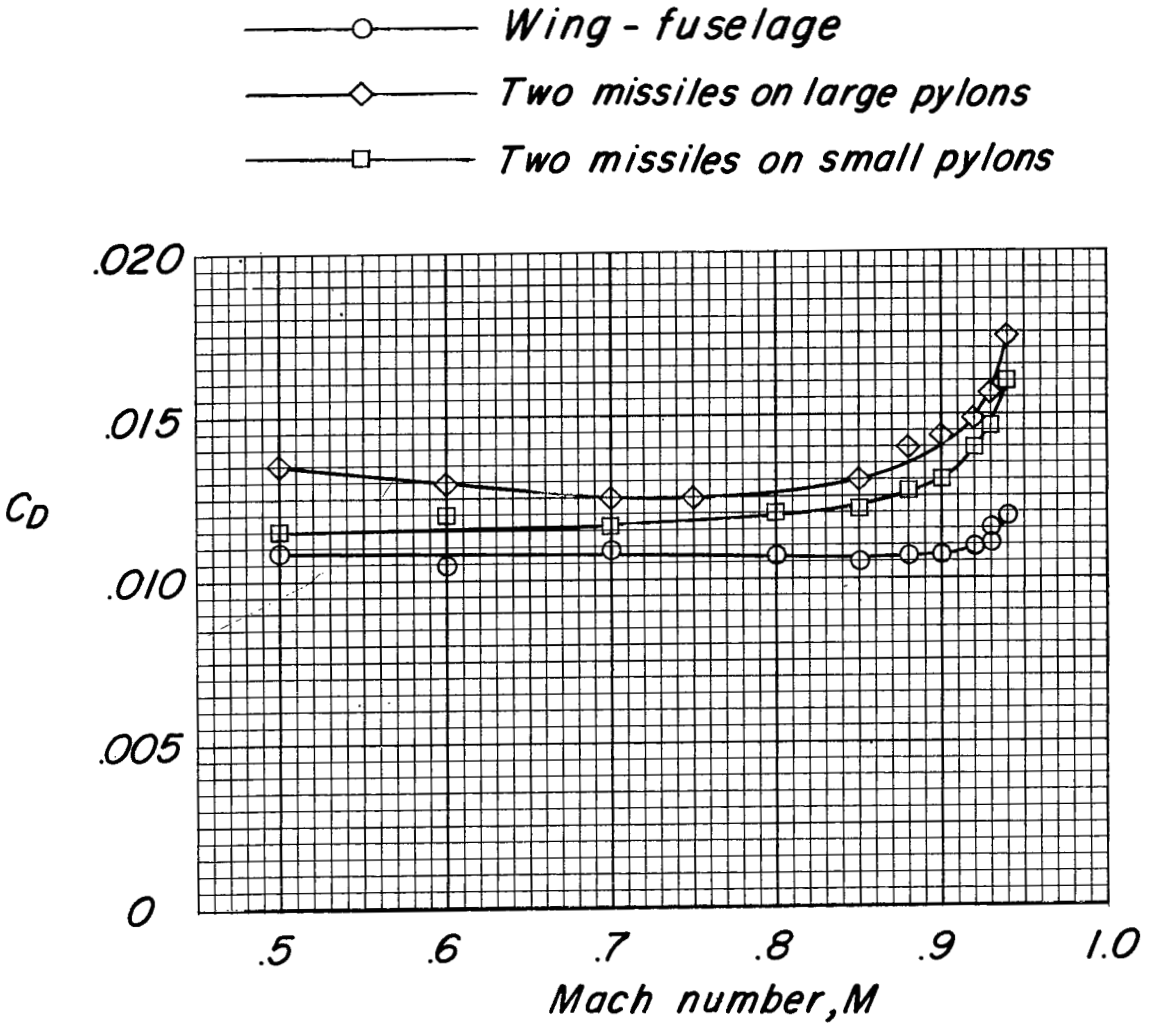

Figure 10.- Variation of drag coefficient with Mach number of model A without and with pylon-mounted missiles. $\alpha = 0^\circ$.

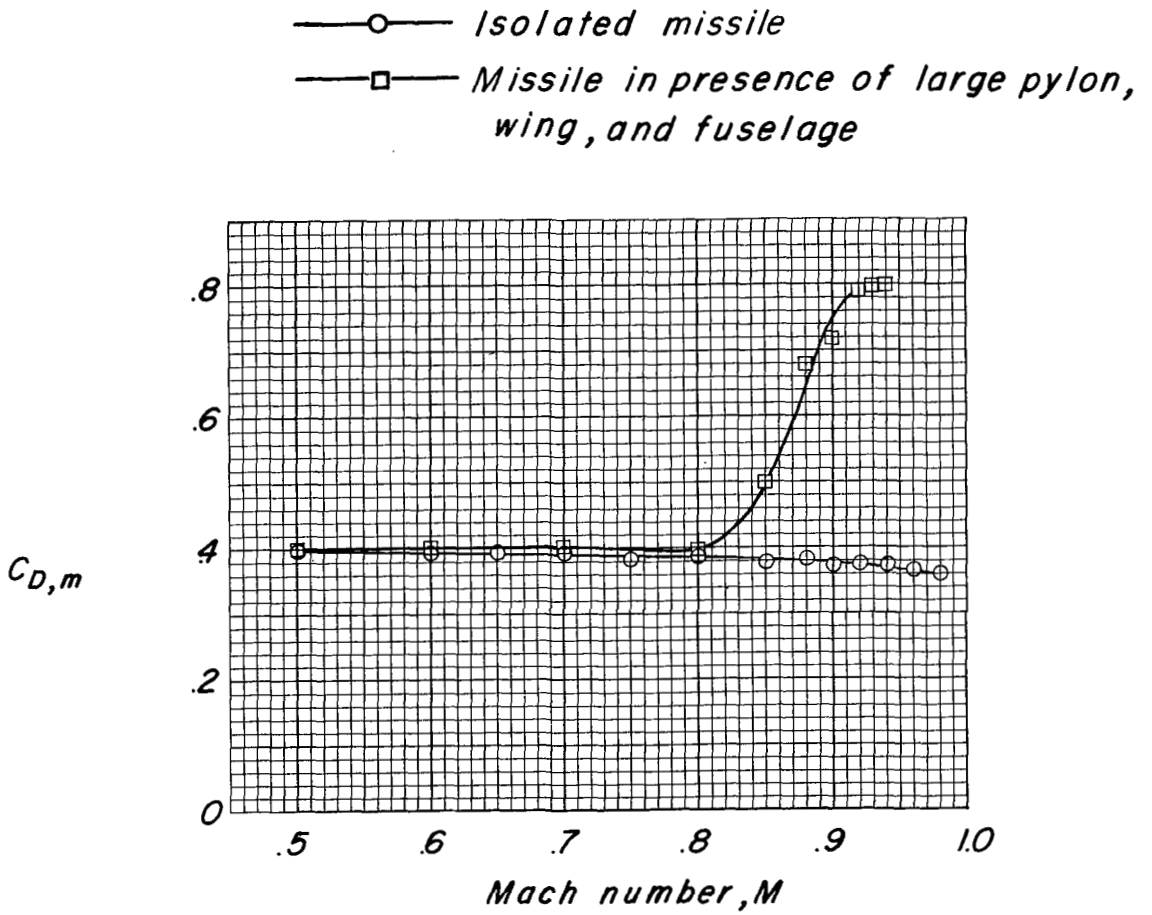

Figure 11.- Variation of drag coefficient with Mach number of isolated missile and missile in presence of large pylon, wing, and fuselage. $\alpha = 0^{\circ}$.

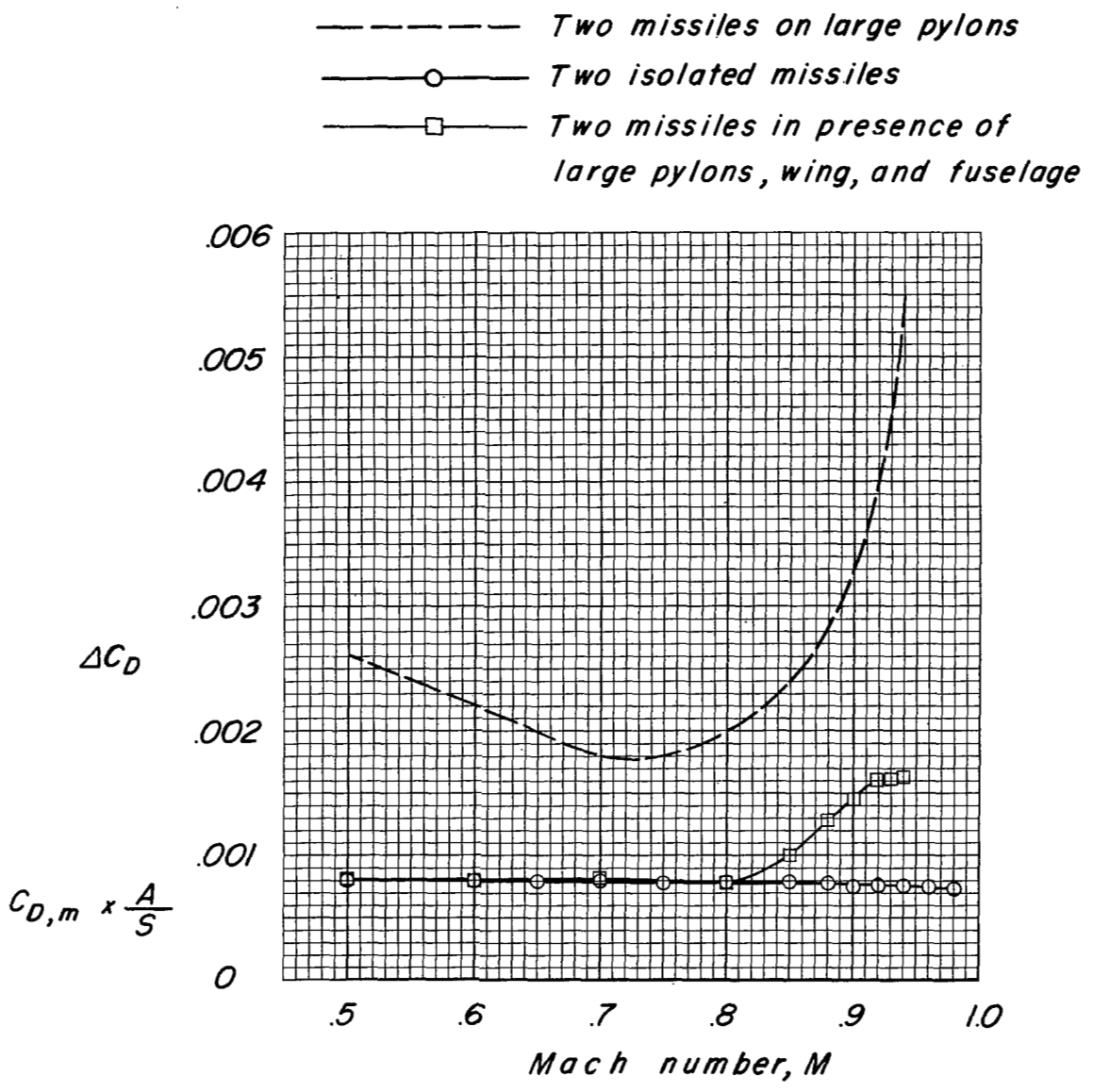

Figure 12.- Comparison of installation drag of two pylon-mounted missiles, drag of two isolated missiles, and twice drag of one missile in presence of large pylon, wing, and fuselage. $\alpha = 0^{\circ}$.

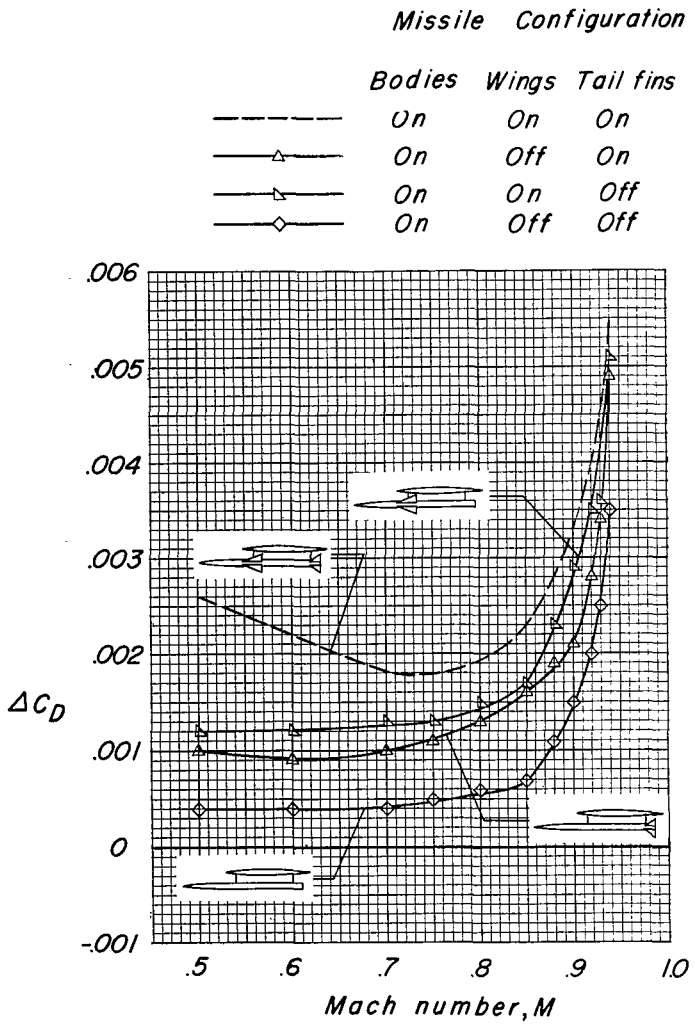

(a) Missile components, large pylons.

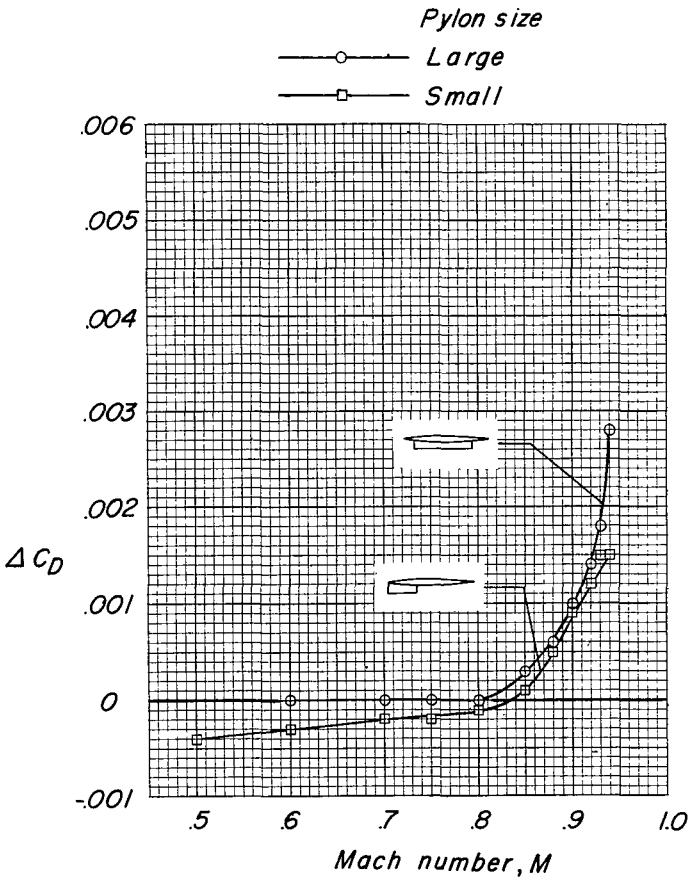

(b) Pylons only.

Figure 13.- Effect of missile components and pylons on installation drag.

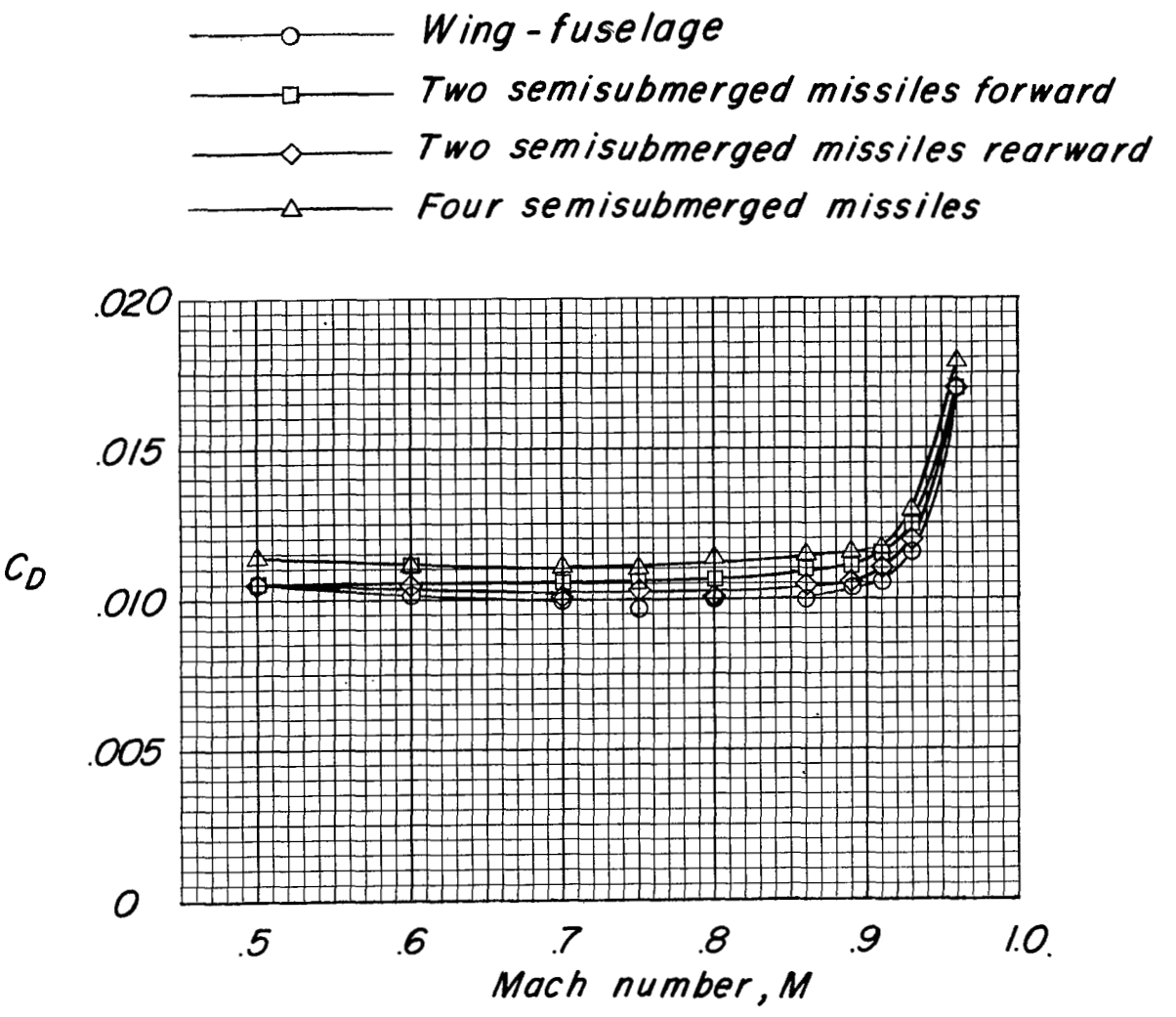

Figure 14.- Variation of drag coefficient with Mach number of model B without and with semisubmerged missiles. $\alpha = .0^\circ$.

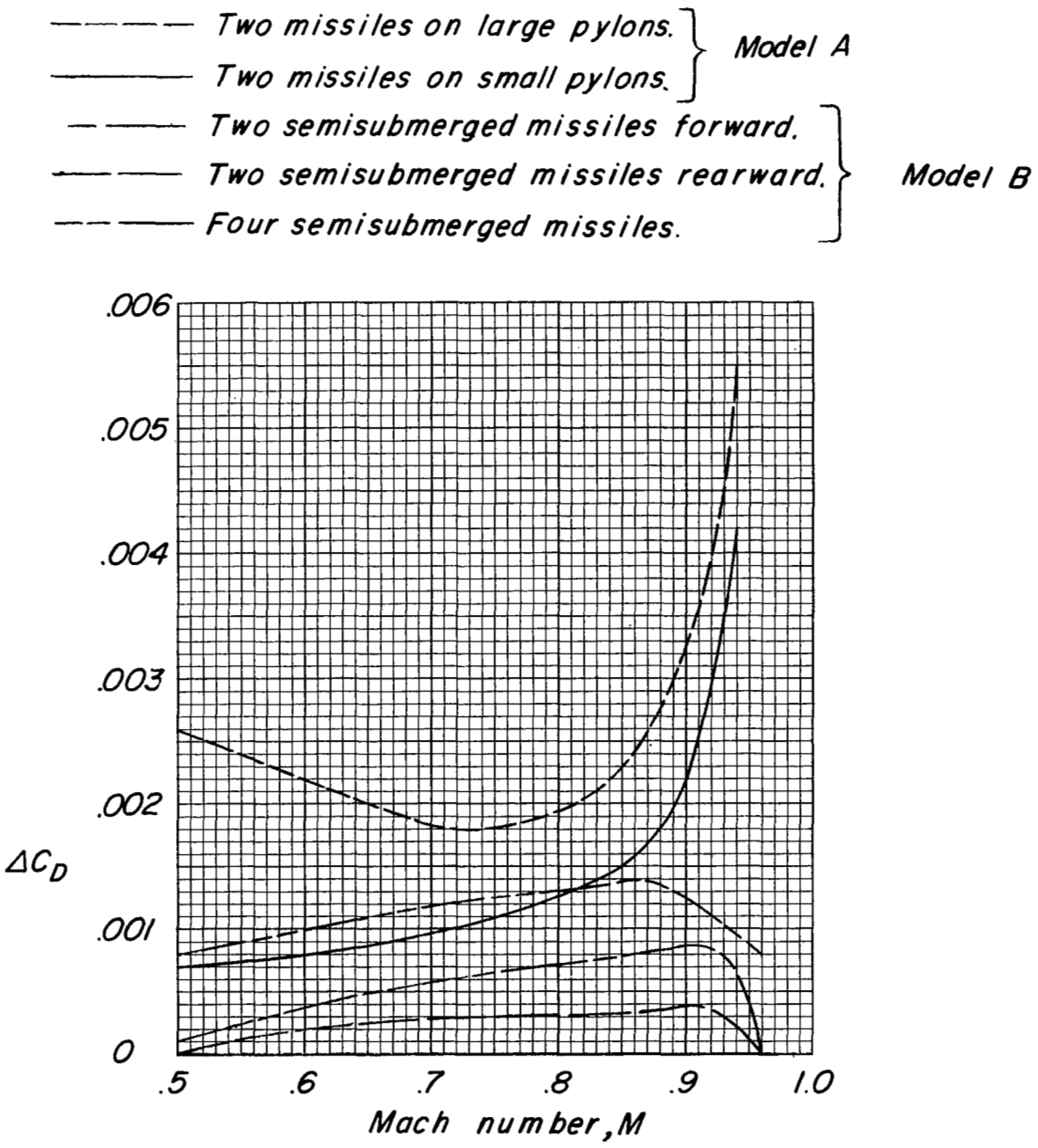

Figure 15.- Comparison of installation drag of pylon-mounted missiles on model A and semisubmerged missiles on model B.

NACA - Langley Field, Va.